Research Paper

Australasian microtektites across the Antarctic continent: Evidence from the Sør Rondane Mountain range (East Antarctica)

Bastien Soens [a,b,*], Matthias van Ginneken [c], Stepan Chernonozhkin [d], Nicolas Slotte [b], Vinciane Debaille [b], Frank Vanhaecke [d], Herman Terryn [e], Philippe Claeys [a], Steven Goderis [a]

[a] Analytical, Environmental, and Geo-Chemistry, Vrije Universiteit Brussel, Pleinlaan 2, BE-1050 Brussels, Belgium
[b] Laboratoire G-Time, Université Libre de Bruxelles 50, Av. F.D. Roosevelt CP 160/02, BE-1050 Brussels, Belgium
[c] Centre for Astrophysics and Planetary Science, University of Kent, CT2 7NZ, Canterbury, Kent, United Kingdom
[d] Atomic & Mass Spectrometry – A&MS Research Unit, Department of Chemistry, Ghent University, Campus Sterre, Krijgslaan 281 – S12, BE-9000 Ghent, Belgium
[e] Electrochemical and Surface Engineering, Vrije Universiteit Brussel, Pleinlaan 2, BE-1050 Brussels, Belgium

ARTICLE INFO

ABSTRACT

The ~790 ka Australasian (micro)tektite strewn field is one of the most recent and best-known examples of impact ejecta emplacement as the result of a large-scale cratering event across a considerable part of Earth's surface (>10% in area). The Australasian strewn field is characterized by a tri-lobe pattern consisting of a large central distribution lobe, and two smaller side lobes extending to the west and east. Here, we report on the discovery of microtektite-like particles in sedimentary traps, containing abundant micrometeorite material, in the Sør Rondane Mountain (SRM) range of East Antarctica. The thirty-three glassy particles display a characteristic pale yellow color and are predominantly spherical in shape, except for a single dumbbell-shaped particle. The vitreous spherules range in size from 220 to 570 μm, with an average diameter of ~370 μm. This compares relatively well with the size distribution (75–778 μm) of Australasian microtektites previously recovered from the Transantarctic Mountains (TAM) and located ca. 2500–3000 km from the SRM. In addition, the chemical composition of the SRM particles exhibits limited variation and is nearly identical to the 'normal-type' (i.e., <6% MgO) TAM microtektites. The Sr and Nd isotope systematics for a single batch of SRM particles ($n = 26$) strongly support their affiliation with TAM microtektites and the Australasian tektite strewn field in general. Furthermore, Sr isotope ratios and Nd model ages suggest that the target material of the SRM particles was composed of a plagioclase- or carbonate-rich lithology derived from a Paleo- or Mesoproterozoic crustal unit. The affiliation to the Australasian strewn field requires long-range transportation, with estimated great circle distances of ca. 11,600 km from the hypothetical source crater, provided transportation occurred along the central distribution lobe. This is in agreement with the observations made for the Australasian microtektites recovered from Victoria Land (ca. 11,000 km) and Larkman Nunatak (ca. 12,000 km), which, on average, decrease in size and alkali concentrations (e.g., Na and K) as their distance from the source crater increases. The values for the SRM particles are intermediate to those of the Victoria Land and Larkman Nunatak microtektites for both parameters, thus supporting this observation. We therefore interpret the SRM particles as 'normal-type' Australasian microtektites, which significantly extend the central distribution lobe of the Australasian strewn field westward. Australasian microtektite distribution thus occurred on a continent-wide scale across Antarctica and allows for the identification of new, potential recovery sites on the Antarctic continent as well as the southeastern part of the Indian Ocean. Similar to volcanic ash layers, the ~790 ka distal Australasian impact ejecta are thus a record of an instantaneous event that can be used for time-stratigraphic correlation across Antarctica.

1. Introduction

Tektites (and their submillimeter analogues microtektites) are natural, SiO_2-rich glasses that form during oblique hypervelocity impact of

asteroidal or cometary bodies with the Earth's surface (e.g., Koeberl, 1994; Artemieva et al., 2002). They are distributed over large geographical areas (>100–1000 km) commonly referred to as 'strewn fields', which have previously been linked to large-scale impact cratering events in North America, Ivory Coast and Central Europe (Glass and Simonson, 2013).

The Australasian strewn field is among the largest (>10% of the Earth's surface) and most recent (788.1 ± 3.0 ka; Schwarz et al., 2016;

Jourdan et al., 2019) impact events on Earth in terms of ejecta material, but no source crater has yet convincingly been identified. The existence of such impact crater is nevertheless supported by the presence of melt layers in Australasian tektites, shock-metamorphic features observed in Australasian tektites, microtektites and microscopic ejecta particles recovered from Australasian ejecta layers, and high pressure-temperature mineral phases, including coesite and reidite in Muong Nong-type tektites (e.g., Walter, 1965; Glass and Wu, 1993; Folco et al., 2010b; Cavosie et al., 2017; Glass et al., 2020; Masotta et al., 2020). Furthermore, a detailed investigation of the moderately (e.g., Ni, Co, Cr) and highly (e.g., Os, Ir, Pt, Pd, Rh, Ru, Re) siderophile element concentrations in Australasian impact ejecta has revealed that their geochemistry is consistent with upper continental crust material to which chondritic or primitive achondritic material was admixed (Goderis et al., 2017; Folco et al., 2018; Ackerman et al., 2019). Based on the distribution and physicochemical properties (i.e., size distribution, composition) of Australasian impact ejecta, it has been suggested that the hypothetical source crater is located on the northern or central parts of the Indochina peninsula (Barnes, 1964; Glass and Pizzuto, 1994; Ma et al., 2004; Prasad et al., 2007; Folco et al., 2010a, 2010b). Based on geophysical evidence, Sieh et al. (2020) have argued that the Australasian impact crater is buried beneath the Bolaven volcanic field in southern Laos. Australasian (micro)tektites are distributed along a tri-lobed pattern consisting of a large, central (SE Asia, Australia) SSE orientated ejecta ray, which is flanked by two smaller, western (Indian Ocean, SE Africa) and eastern (Pacific Ocean) side lobes (Fig. 1). This distinctive lobe pattern was reconstructed through multiple (>60) ocean drilling program (ODP) campaigns and other oceanographic studies, revealing the location of Australasian (micro)tektites distributed on the seafloor of the Indian and Pacific Oceans (Glass and Simonson, 2013).

Microtektites have previously been recovered from sediment traps on nunataks (e.g., Miller Butte, Pian delle tectiti, etc. – Victoria Land)

and glacial moraines (e.g., Larkman Nunatak) in the TAM (Folco et al., 2008, 2009, 2016; van Ginneken et al., 2018) (Fig. 1). Due to the isolated nature and high altitude ca. 2600–2800 m.a.s.l.) of these sampling sites, the accumulation of material is restricted to surrounding basement rock and direct atmospheric infall, including micrometeorites, volcanic glass shards, meteorite ablation debris, and microtektites (e.g., Folco et al., 2008, 2009; Rochette et al., 2008; van Ginneken et al., 2010). Major and trace element compositions of the Victoria Land microtektites are consistent with those of microtektites at other sites within the Australasian strewn field. However, their volatile compounds (e.g., Na_2O, K_2O) are strongly depleted and presumably record a high degree of vaporization, which is compatible with large-scale translation from the source crater (Artemieva et al., 2002; Folco et al., 2010a; van Ginneken et al., 2018). Isotopic tracers ($^{87}Sr/^{86}Sr$ and $^{143}Nd/^{144}Nd$) have provided an unequivocal link to the Australasian impact event, demonstrating that the Victoria Land and Australasian microtektites have sampled similar target rocks (Folco et al., 2009). Fission track dating also confirms similar formation ages (ca. 0.85 ± 0.17 Ma) that match the Australasian impact event (Folco et al., 2011), effectively extending the central distribution lobe of the Australasian strewn field approximately 3000 km southward.

Here, we report the discovery of thirty-three microtektite-like particles from sedimentary traps in the Sør Rondane Mountain range (East Antarctica). We present major, trace element and Sr–Nd isotope data to determine the nature of the SRM particles and compare them to other Antarctic microtektites, previously affiliated to the Australasian strewn field. The implications of such potential affiliation are threefold: (1) the geographical distribution of Australasian microtektites can be refined and allows for new, potential recovery sites to be identified, (2) this information, in turn, is relevant to reconstruct the collisional parameters (e.g., entry angle, direction) of the hypervelocity bolide impact and refine the target stratigraphy, and (3) the abundance and
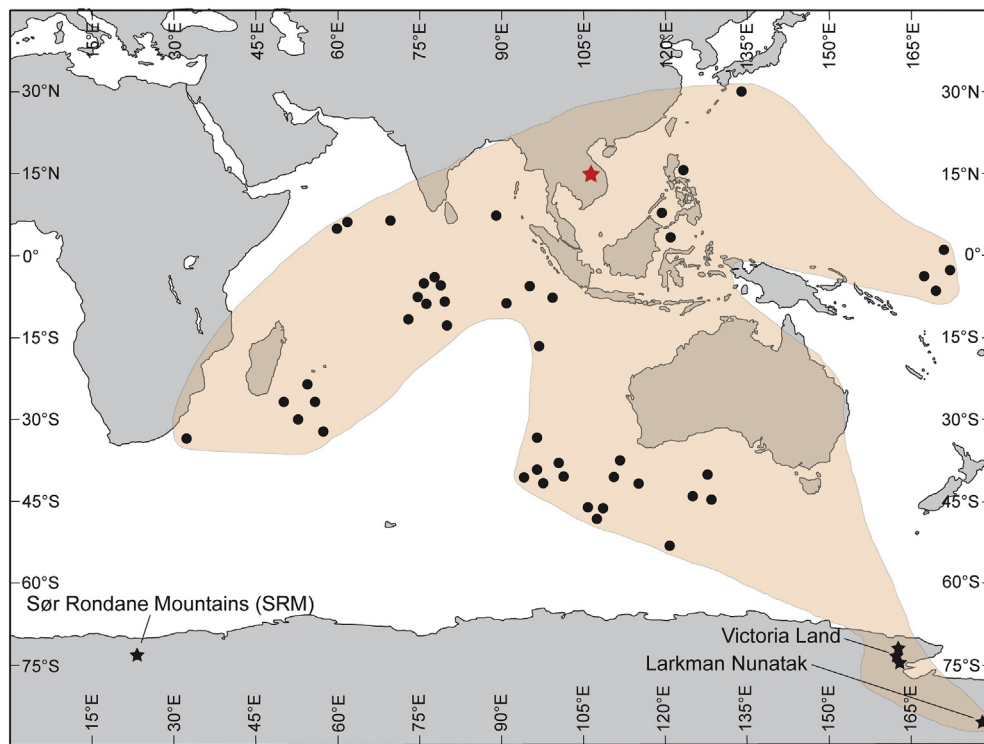

Fig. 1. Geographical distribution (contour) of the recovery sites (ODP - black filled circles) of Australasian (micro)tektites with indication of the Sør Rondane (SRM) and Transantarctic Mountain ranges, including the Victoria Land and Larkman Nunatak sampling sites. Note that continental recovery sites (e.g., Indonesia, Laos, Australia, etc.), except for those on the Antarctic continent, are not shown here. The SRM and TAM chains are separated approximately 2500–3000 km from one another. The hypothetical crater location (star symbol) is based on previous suggestions by Barnes (1964), Glass and Pizzuto (1994), Ma et al. (2004), Prasad et al. (2007), Folco et al. (2010a, 2010b), Sieh et al. (2020). Figure modified from Folco et al. (2009, 2016).

preservation potential of microtektites in Antarctic sedimentary traps can be evaluated to increase the chances of success during future sampling campaigns.

2. Materials and methods

A limited number ($n = 33$) of microtektite-like particles has been recovered from sedimentary traps (e.g., exposed cracks, fissured surfaces, moraines) in the SRM, Queen Maud Land, East Antarctica (Figs. 1 and 2; Goderis et al., 2020). These sedimentary deposits were collected during the 2018 Belgian Antarctic Meteorites and Micrometeorites (BAMM!) expedition. Based on the bedrock exposure ages and general glacial history for the western part of the SRM, accumulation of extraterrestrial- and impact-related material presumably occurred over a time span of ~1–3 Ma at the respective sampling sites (Suganuma et al., 2014). Accumulation appears to be directly controlled by atmospheric infall as demonstrated for the Mt. Widerøe cosmic spherule collection, based on the structural, textural, chemical, and isotopic characteristics of this collection (Goderis et al., 2020).

Bulk sedimentary deposits were weighed and wet-sieved into six different size fractions ranging from <125 μm up to >2000 μm. The deposit was subsequently dried in an oven for 12 h at a temperature of ca. 60 °C. Microtektites were mainly searched for in the non-magnetic size fractions between 200 and 800 μm. The separation of magnetic particles was performed by repeatedly moving a hand magnet over the respective size fractions until no additional material remained attached to the magnet. Potential microtektite particles were then manually extracted using a set of titanium tweezers and binocular microscope. Semi-quantitative geochemical compositions were determined using a JEOL JSM IT-300 scanning electron microscope (SEM), coupled to an Oxford energy dispersive spectrometer (EDS) at the SURF department of the Vrije Universiteit Brussel (Brussels, Belgium). Operating conditions for SEM analysis were 15 kV acceleration voltage and a 10 nA beam current. Given the vitreous nature of the particles, a defocused beam with a ca. 10 μm spot size was used for chemical analysis. The first seven particles, with major element compositions comparable to those of Victoria

Land microtektites, were embedded in epoxy resin and polished for further analysis. An additional 26 particles were placed on a separate glass slide, characterized for major and trace element compositions, and finally combined for Sr and Nd isotope analysis.

Following a short pre-ablation run to clean the exteriors of the particles, the major and trace element compositions of 34 possible microtektites were measured using a Teledyne Cetac Technologies Analyte G2 excimer-based laser ablation system equipped with HelexII double volume cell and ARIS aerosol introduction system and coupled to a Thermo Scientific Element XR sector field inductively coupled plasma – mass spectrometer (LA-ICP-MS) at the Department of Chemistry of the Ghent University (Ghent, Belgium) using an external calibration by USGS and MPI-DING glass reference materials and established sum normalization data processing approach (see Das Gupta et al., 2017; Appendix A, Supplementary Data). Two replicate analyses with a spot size of ca. 35 μm were performed on the first seven microtektite candidates, while the remaining 26 bulk particles were analyzed two to three times using a 40 μm circular spot size, depending on their size. During these analyses, a single vitreous cosmic spherule was identified among the selected particles and excluded from the following analyses. In addition, a single green, irregular-shaped vitreous particle was discovered that was subsequently identified as volcanic glass. The accuracy of the LA-ICP-MS analysis was determined by comparing the average bias between the experimentally obtained values and the reference values and was found to be less than 10% for all reported elements. To determine the reproducibility of the applied procedure, the relative standard deviation (RSD) was calculated for the MPI-DING ATHO-G reference glass. For most elements, the reproducibility was ≤5% RSD, except in the case of Li, Ge, As, Mo, Cs, Tb, Tm (5%–10% RSD), and Be, Cr, Co, Ni, Sb, U (>10% RSD). The slightly worse reproducibility of the latter elements can be attributed to their lower concentration in the ATHO-G reference glass. This is furthermore supported by their good reproducibility (<10% RSD) in other USGS and MPI-DING reference glasses such as BHVO-2G and ML3B-G, where these respective elements are more concentrated.
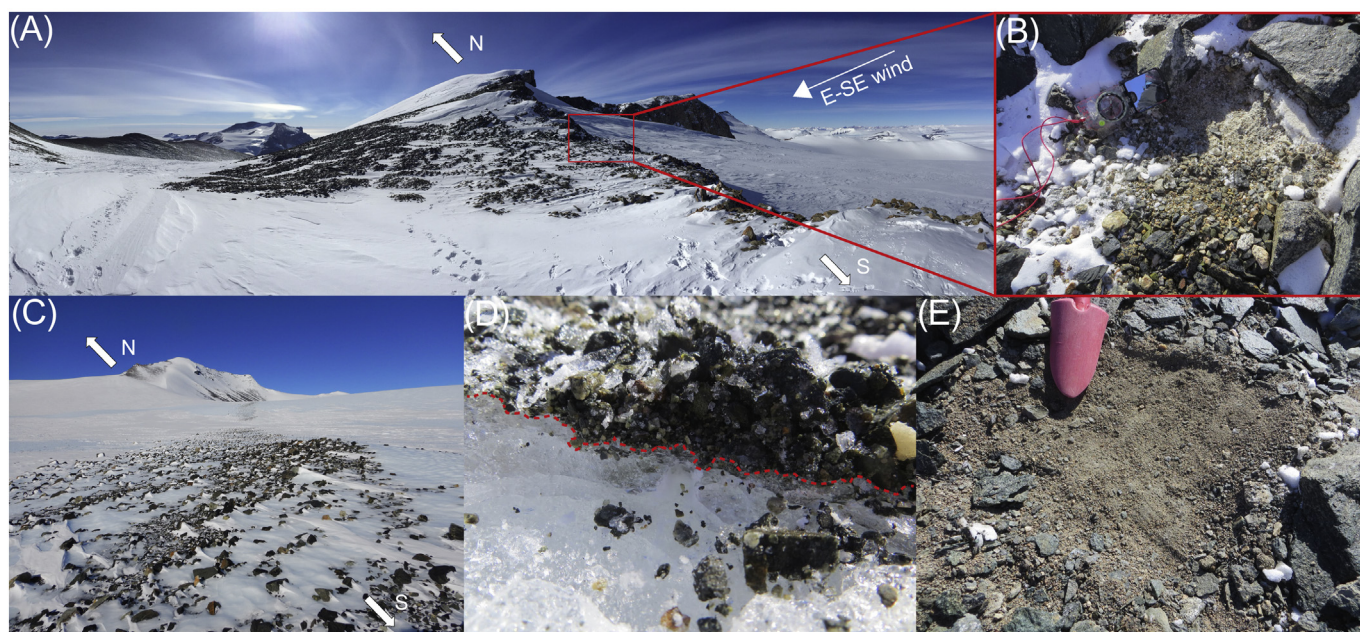

Fig. 2. Overview of the sampling locations in the Sør Rondane Mountains. (A) Overview of the Mt. Widerø summit with indication of the Mt. Widerø #1 sampling location (window – S72.14458°, E23.27798°). (B) Detailed view upon the Mt. Widerø #1 sedimentary trap with compass for scale. (C) Moraine deposits near the Mt. Walnum summit. (D) Detailed view upon the Walnumfjellet Moraine sedimentary trap (S72.13632°, E23.84309°) illustrating the incorporation of moraine deposits in the ice sheet. The dashed line indicates the transition from the sediment to ice. (E) Detailed view upon the Mt. Walnum #1 sedimentary trap (S72.10801°, E24.22434°) with scoop for scale. The sedimentary traps are located at elevations between ca. 2500–2800 m.a.s.l. and are continuously subjected to frosty conditions.

For Sr–Nd isotope measurements, 0.8 mg of combined microtektites, alongside with USGS international standards BCR-2 (2 mg) and BHVO-2 (1 mg), was dissolved using subboiled 3:1 HNO_3 : HF for 2 days at 120 °C, and subboiled HCl after evaporation for one day at 120 °C at the Laboratoire G-Time at the Université Libre de Bruxelles (Brussels, Belgium). Cationic resin has been used to separate Sr in 1.5 N HCl from rare earth elements (REE) in 6 N HCl. Strontium has subsequently been purified, notably from Rb, by using Sr.Spec resin in combination with 7 N HNO_3, while Nd has been purified from other REE, and notably Sm, using HDEHP resin with 0.16 and 0.27 N HCl. Both Sr and Nd isotope compositions have been measured on the Nu-Plasma2 multi-collection inductively coupled plasma-mass spectrometer at Laboratoire G-Time using a desolvating nebulizer Aridus 2 system. For Sr, the NBS987 standard was measured at 50 ppb, and provided an average value of $^{87}Sr/^{86}Sr = 0.710372 \pm 0.000019$ ($2\sigma, n = 20$), and values were subsequently corrected with the accepted value by standard-bracketing at $^{87}Sr/^{86}Sr = 0.710248$ (Weis et al., 2006). Internal reproducibility based on repeated measurement of an in-house carbonate standard ($n = 4$) is better than 35 ppm (2σ). For Nd, the Rennes standard was measured at 10 ppb and yielded an average value of $^{143}Nd/^{144}Nd = 0.511951 \pm 0.000035$ ($2\sigma, n = 15$), and values were corrected for the accepted value by standard-bracketing at $^{143}Nd/^{144}Nd = 0.511963$ (Chauvel and Blichert-Toft, 2001). Internal reproducibility based on repeated analysis of the JMC quality control standard ($n = 3$) is better than 35 ppm and is identical to the value obtained for 15 Rennes standards. In both cases, BCR-2 and BHVO-2 values overlap within error with published values (e.g. Weis et al., 2006).

3. Results

In total, thirty-three glassy spherules were identified as microtektites in the SRM deposits using SEM-EDS and LA-ICP-MS analysis based on their Si-Al-enriched composition ($SiO_2 = 65.2$–76.1 wt.%, $Al_2O_3 = 12.2$–20.1 wt.%), which distinguishes them from chondritic (vitreous) cosmic spherules (Figs. 3 and 4 and Appendix A, Supplementary Data). Additionally, their volatile element concentrations (e.g., Na_2O, K_2O) are significantly higher than those of (a)chondritic micrometeorites, but lower than those of Victoria Land volcanic glass shards and the single volcanic glass particle recovered during this study (Fig. 3). The SRM particles therefore discriminate themselves from all types of (extra)terrestrial materials recovered from Antarctic

micrometeorite traps, except for the TAM microtektites (Folco et al., 2009). Their major element compositions also fall within the compositional range defined by 'normal-type' (<6 wt.% MgO) Australasian microtektites and, more specifically, overlap with the compositions of the 'normal-type' Victoria Land microtektites (Glass et al., 2004; Folco et al., 2008, 2009, 2016; see Figs. 3 and 4). No other chemical microtektite types (i.e., intermediate, high-Mg, high-Al, or high-Ni, Fe-type; Glass et al., 2004; Folco et al., 2016, 2018) have been recovered from the SRM collection so far.

The trace element compositions, including the refractory elements Zr and Hf, are consistent with 'normal-type' Victoria Land microtektites (Fig. 5). Zinc is the sole exception and appears to be notably depleted in the SRM particles. Additionally, three samples, which are indistinguishable from the other SRM particles based on major element geochemistry, extend the known ranges in V, Cs, Pb and U contents. The multi-element diagram displays the range of elemental concentrations observed in the characterized particles and are normalized to upper continental crust values (Taylor and McLennan, 1995) (Fig. 6). Their geochemical composition strongly resembles the pattern defined by 'normal-type' Victoria Land microtektites, with concentrations similar to those of the upper continental crust, except for Na, K, V, Zn, Cs, Pb and U, which are strongly depleted relative to crustal values.

The $^{143}Nd/^{144}Nd$ ratio (0.512073 ± 10, 2σ) of the SRM particles is identical (within error) to that measured for Victoria Land microtektites (0.512086 ± 29, 2σ), and is fully consistent with the Australasian strewn field. In contrast, the $^{87}Sr/^{86}Sr$ ratio (0.716664 ± 12, 2σ) is within range of the values observed for Victoria Land microtektites (0.716215 ± 10, and 0.716372 ± 10, 2σ), but offset to slightly higher values in the direction of Australasian tektites from Malaysia, China and the Philippines. Isotopic ratios in Fig. 7A are expressed in the ε notation, where $\varepsilon = [(R_{sample} - R_{standard})/R_{standard}] \times 10,000$. The reference material used for comparison of the Sr and Nd isotopes are Uniform Reservoir (UR) and Chondritic Uniform Reservoir (CHUR), respectively. This translates to $\varepsilon^{87}Sr_{UR}$ and $\varepsilon^{143}Nd_{CHUR}$ values of 173 and -11.0, respectively, for the SRM particles. This compares well with the values observed for Victoria Land microtektites ($\varepsilon^{87}Sr_{UR} = 166$–168, $\varepsilon^{143}Nd_{CHUR} = -10.8$) (Table 1; Folco et al., 2009). The single and two-stage Nd model ages, calculated with respect to the Depleted Mantle (DM) reservoir, are consequently also highly comparable between the SRM particles and Victoria Land microtektites (Table 1), and are
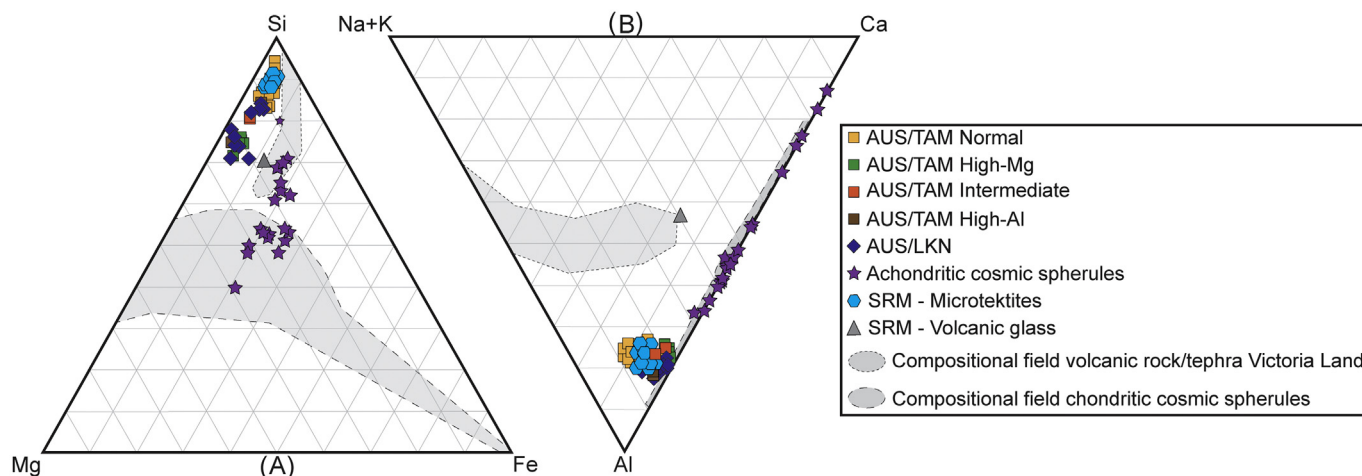

Fig. 3. Ternary diagrams discriminating chondritic and achondritic micrometeorites, Australasian microtektites and volcanic rocks-tephra from Victoria Land (Antarctica) based on the distribution of Si-Fe-Mg (A) and Al-Ca-Na-K (B). Values are calculated based on the atomic abundances of elements (see Appendix A, Supplementary Data). In both instances, the SRM particles are positioned within the range defined by 'normal-type' Australasian microtektites from the Transantarctic Mountains (TAM). A single, green irregular-shaped glass particle is presumably linked to volcanic activity in Victoria Land and is referred to as 'SRM – Volcanic Glass'. Reference values for Australasian microtektites, (a)chondritic micrometeorites and volcanic rock-tephra reproduced from Perchiazzi et al. (1999), Taylor et al. (2007), Curzio et al. (2008), Rochette et al. (2008), Folco et al. (2009), Cordier et al. (2011, 2012) and van Ginneken et al. (2018). Figure modified from Folco et al. (2009).
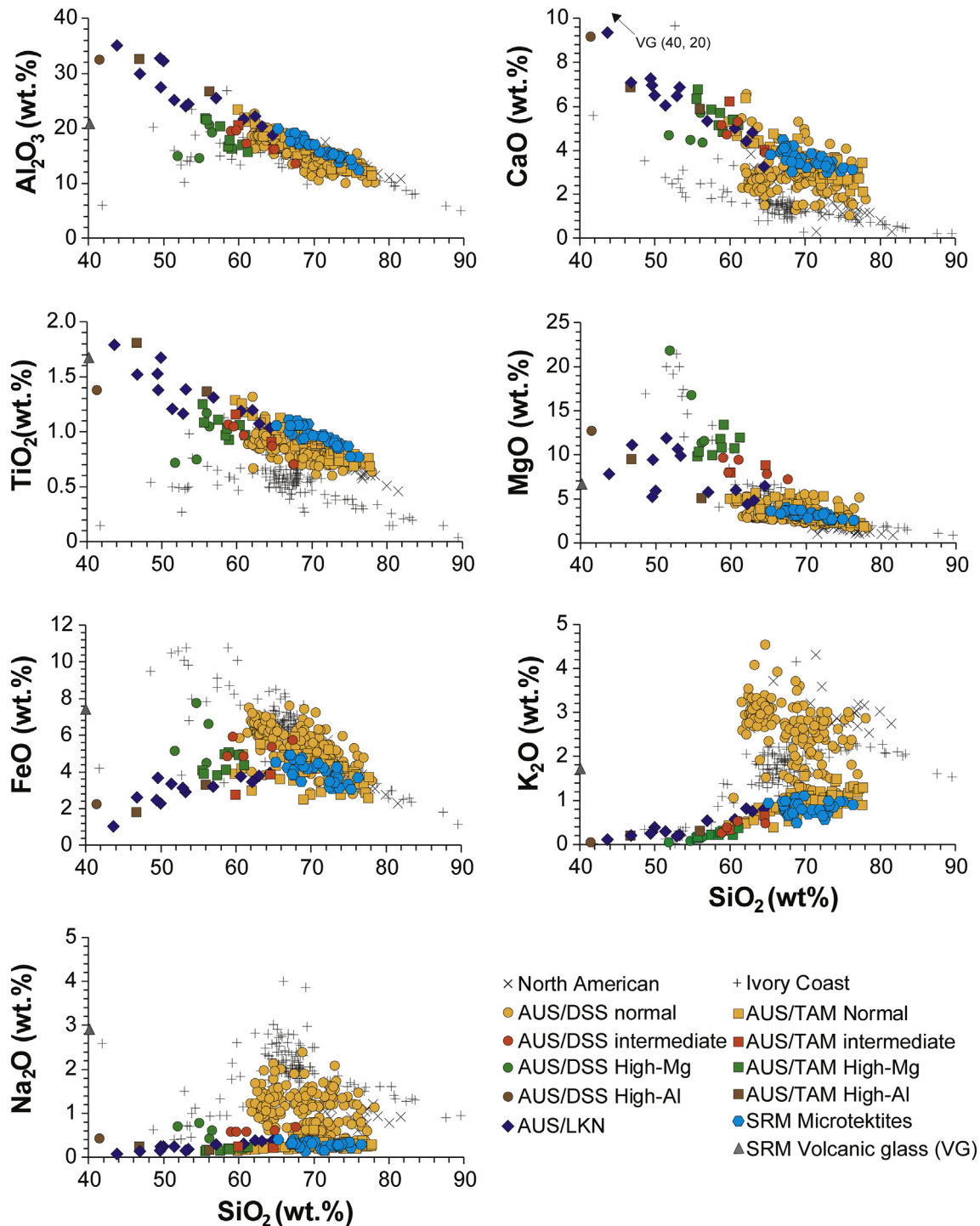
Fig. 4. Major element chemistry of the SRM particles (including a single volcanic glass particle – VG) determined by LA-ICP-MS (see Appendix A, Suplementary Data). The geochemical range of the particles is largely indistinguishable from reference values for Victoria Land (TAM) microtektites and is clearly distinguished from the volcanic glass particle. Reference values for North American, Ivory Coast and Australasian (micro)tektites (DSS – Deep Sea Sediment) were reproduced from Glass et al. (2004), Folco et al. (2009, 2016) and van Ginneken et al. (2018). Figure modified from van Ginneken et al. (2018).

consistent with reference values for Australasian tektites (Folco et al., 2009; Ackerman et al., 2020). This age indicates the time at which the parent material of the respective particles physicochemically separated from the DM reservoir. However, the single-stage model assumes that the parent material of the SRM and TAM particles directly separated from the DM reservoir, while the two-stage model assumes that the crustal unit is composed of recycled, well-mixed sedimentary strata.

The single-stage model age for the SRM particles indicates a possible Mesoproterozoic age, while the two-stage model age is slightly older suggesting a Paleo- or Mesoproterozoic age. Furthermore, on a diagram of $^{87}Sr/^{86}Sr$ versus $1/Sr$, which indicates a mixing of Sr-rich and Sr-poor isotopically distinct components, the SRM particles and Victoria Land microtektites plot within the 'normal and intermediate australites' field (Fig. 7B). Both groups of particles also display $^{87}Sr/^{86}Sr$ ratios
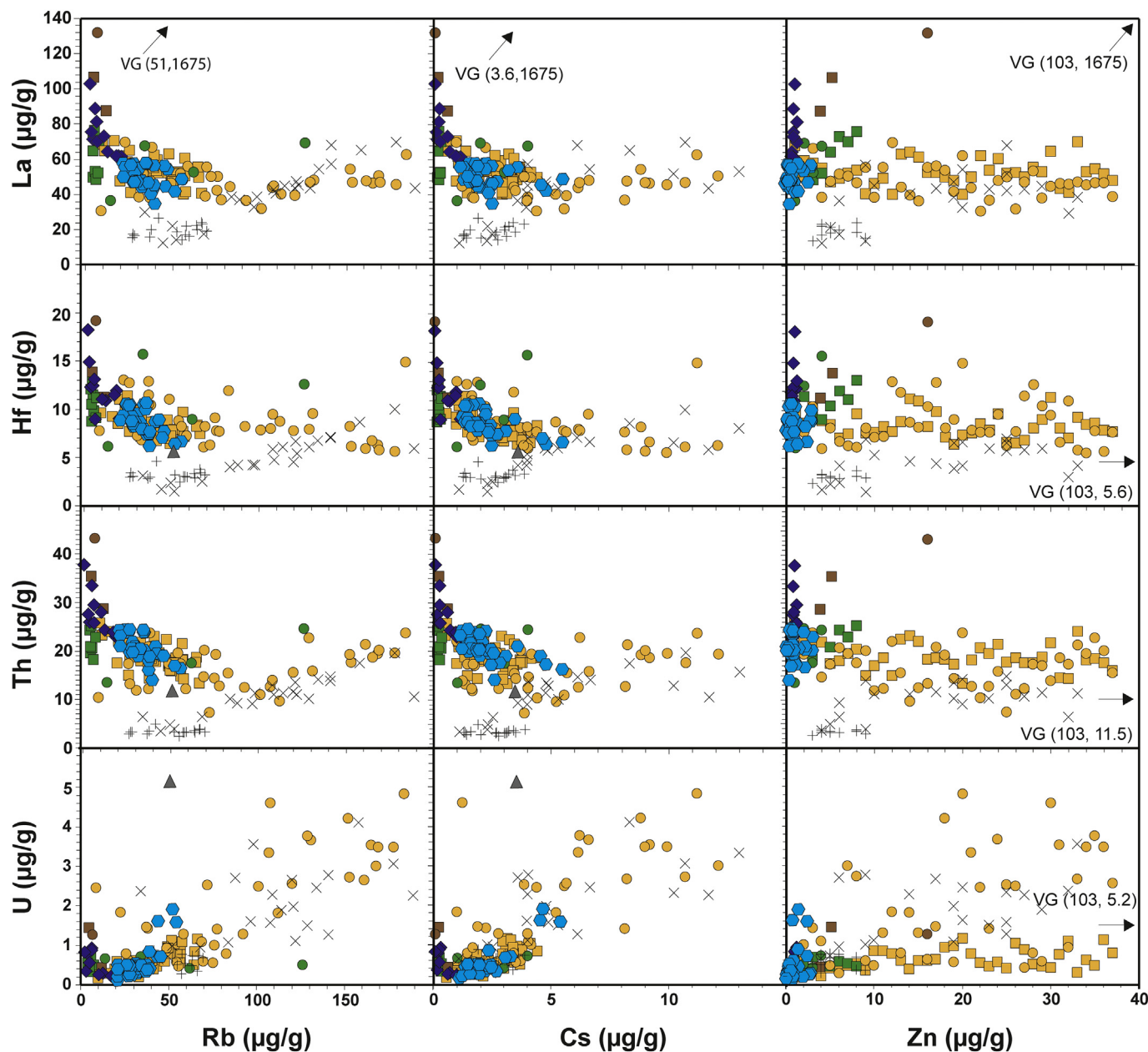
Fig. 5. Trace element geochemistry of the SRM particles (including a single volcanic glass particle – VG) determined by LA-ICP-MS (see Appendix A, Supplementary Data). Particles are predominantly positioned within the geochemical range defined by the Victoria Land (TAM) microtektites, except for Zn. Three samples within the SRM suite are characterized by higher Cs and U contents. The reader is referred to Fig. 4 to observe the legend of this figure. Reference values for North American, Ivory Coast and Australasian (micro)tektites are from Glass et al. (2004), Folco et al. (2009, 2016) and van Ginneken et al. (2018). Figure modified from van Ginneken et al. (2018).

similar to those observed in splash-form Australasian tektites from Indonesia and the Philippines, but at lower K_2O/CaO values (Fig. 7C).

The pale yellow, transparent SRM particles range in size between ca. 224 and 568 μm and are predominantly spherical in shape (ca. 97%) (Fig. 8). A single particle displays a more irregular and flattened morphology. We refer to this particle as 'dumbbell-shaped'. The major and trace element composition of the dumbbell-shaped particle does not exhibit notable differences compared to its spherical counterparts. No vesicles were observed during petrographic and SEM analysis. The size distribution of the SRM particles is not well constrained due to the relatively limited sample set ($n = 33$). The peak area is distributed between ca. 300 and 500 μm with an average size of ca. 378 μm. This is positioned in between the average sizes of Australasian microtektites recovered

from Larkman Nunatak (ca. <300 μm) and Victoria Land (ca. 500 μm) (Folco et al., 2008, 2009, 2016; van Ginneken et al., 2018).

4. Discussion

4.1. Nature of the Sør Rondane Mountain particles

The physicochemical properties and Sr–Nd isotopic compositions of the SRM particles bear a strong resemblance with 'normal-type' Victoria Land microtektites (Folco et al., 2008, 2009, 2016), and Australasian tektites as a whole (Glass et al., 2004). The Australasian impact event has previously been dated to ca. 788.1 ± 2.8 ka (Schwarz et al., 2016; Jourdan et al., 2019), which is considerably younger than the final
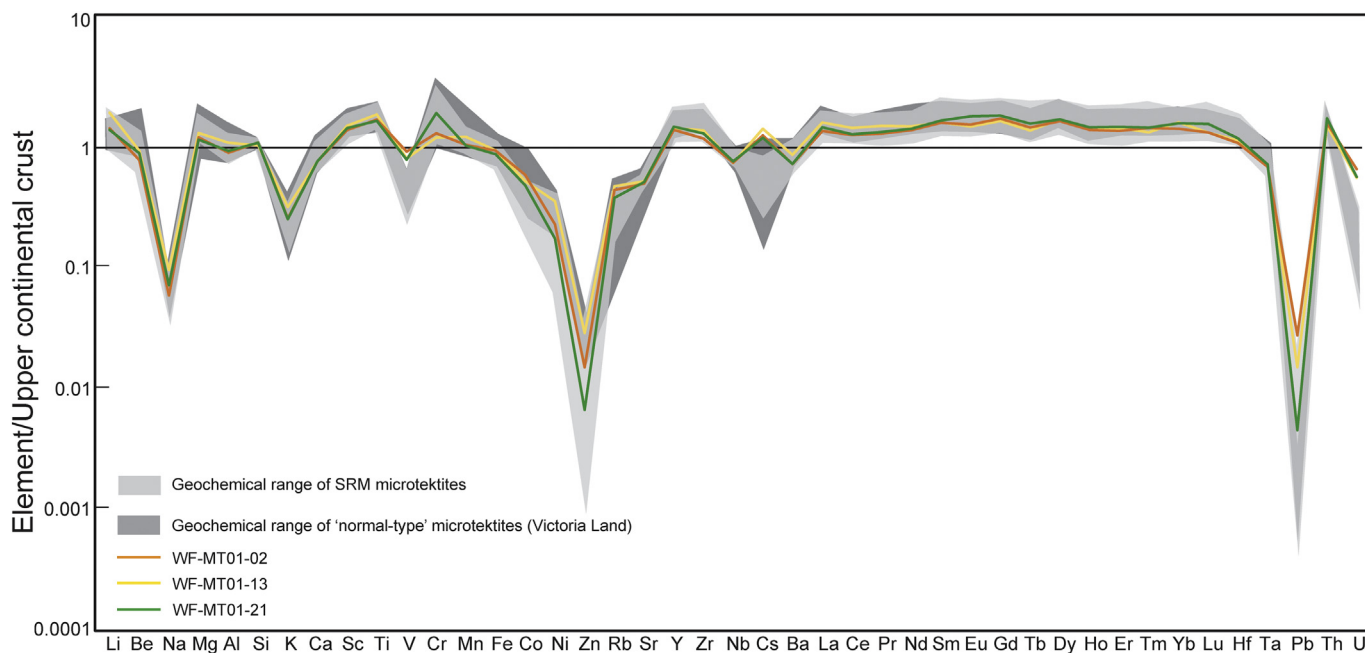
Fig. 6. Geochemical plot of major and trace element chemistry normalized against average compositions of the upper continental crust. The light grey envelope represents the compositional range of the SRM particles (see Appendix A, Supplementary Data), while the dark grey envelope represents the compositional range of 'normal-type' microtektites from the Victoria Land (TAM) (Folco et al., 2009). The three distinct lines represent individual SRM microtektites that slightly extend the range for V, Pb, U, and Cs. Reference values for upper continental crust and Victoria Land microtektites are from Taylor and McLennan (1995) and Folco et al. (2009), respectively. Figure modified from Folco et al. (2009).

deglaciation stages of the SRM (ca. 1–3 Ma; Suganuma et al., 2014). As such, there is a possibility that the SRM sedimentary traps were able to collect Australasian microtektites. To confirm the nature of the SRM particles as (Australasian) microtektites, several key properties need to be verified (Koeberl, 1994; Montanari and Koeberl, 2000; Glass and Simonson, 2013): (i) distribution over a large geographical area, (ii) aerodynamic shapes due to the molten state of the precursor material during atmospheric transportation, (iii) major and trace element geochemistry resembling average compositions of the upper continental crust, (iv) the presence of high SiO_2 (lechatelierite) inclusions, and (v) relatively low H_2O contents.

(i) Large impact cratering events commonly produce an ejecta curtain consisting of e.g., tektites, microtektites, clinopyroxene-bearing spherules, which are transported ca. 100 s to 1000 s of kilometers from the source crater (Glass et al., 2004). Despite the substantial distance between the SRM and TAM ranges (ca. 2500–3000 km), we have observed nearly identical physicochemical features between both types of particles, suggesting they have shared a common source lithology. A contribution of volcanic rock or tephra can be excluded based on their major and trace element chemistry, which is characterized by higher CaO, Na_2O, K_2O and LREE contents with respect to the SRM particles and Victoria Land microtektites (Figs. 3–5).

The sampling sites of the Victoria Land and Larkman Nunatak microtektites are located at ca. 11,000 and 12,000 km from the hypothetical source crater in Indochina, respectively. Following the distribution of Australasian impact ejecta (Fig. 1), the SRM particles may have travelled along the central or western distribution lobe. However, this would greatly affect the total travel distance of the SRM particles. If transportation occurred along the central distribution lobe, then the estimated great circle distance would amount ca. 11,600 km. Alternatively, the estimated great circle distance would exceed ca. 13,000 km if transportation occurred along the western distribution lobe instead.

Folco et al. (2010a) observed that the concentration of volatile compounds (e.g., Na_2O, K_2O) in Australasian (micro)tektites is inversely correlated with distance from the hypothetical source crater (Fig. 9A). They have attributed this observation to high-temperature vaporization of

crustal target rocks during oblique hypervelocity impacts. According to Artemieva et al. (2002), heating temperatures systematically increase closer to the point of impact, severely depleting volatile components, reducing the overall size of microtektites due to a reduction in surface tension processes, and limiting the presence of high SiO_2 inclusions and vesicles. This hypothesis is consistent with mathematical models of Melosh (1989), who suggested that impact ejecta, which originated closer to the contact surface, are subjected to more extreme pressure-temperature conditions and are thus ejected further away from the source crater. This would imply that the translational history of Australasian (micro)tektites is possibly correlated to a number of criteria including volatile element depletion, size-frequency distribution, and the presence of high SiO_2 inclusions and vesicles.

The concentration of volatile compounds ($Na_2O = 0.15$–0.41 wt.%; $K_2O = 0.49$–1.10 wt.%) in the SRM particles are intermediate between the Victoria Land ($Na_2O = 0.15$–0.63 wt.%; $K_2O = 0.38$–1.54 wt.%) and Larkman Nunatak ($Na_2O = 0.07$–0.39 wt.%; $K_2O = 0.10$–0.81 wt.%) microtektites (Folco et al., 2008, 2009, 2016; van Ginneken et al., 2018) (Fig. 9A). The geochemical signatures of the Larkman Nunatak microtektites are more refractory and display greater volatile element depletions compared to 'normal-type' Victoria Land microtektites (van Ginneken et al., 2018), therefore extending the volatilization trend previously established by Folco et al. (2010a). While inconclusive, the intermediate values observed in the SRM particles are supportive of transportation along the central distribution lobe since the extent of volatile element depletion does not exceed that observed in the more refractory Larkman Nunatak microtektites (Fig. 9A).

Following mathematical models (Melosh, 1989; Artemieva et al., 2002) and previous observations (Folco et al., 2009; van Ginneken et al., 2018) regarding the physicochemical properties of microtektites, the size-frequency distribution of microtektites may provide additional insight into the trajectory path followed by the SRM particles. Van Ginneken et al. (2018) have, on average, reported smaller particle sizes (mean diameter of ca. 275 μm) and a narrower size-frequency distribution compared to the Australasian microtektites recovered from Victoria Land (mean diameter of ca. 500 μm). The latter authors
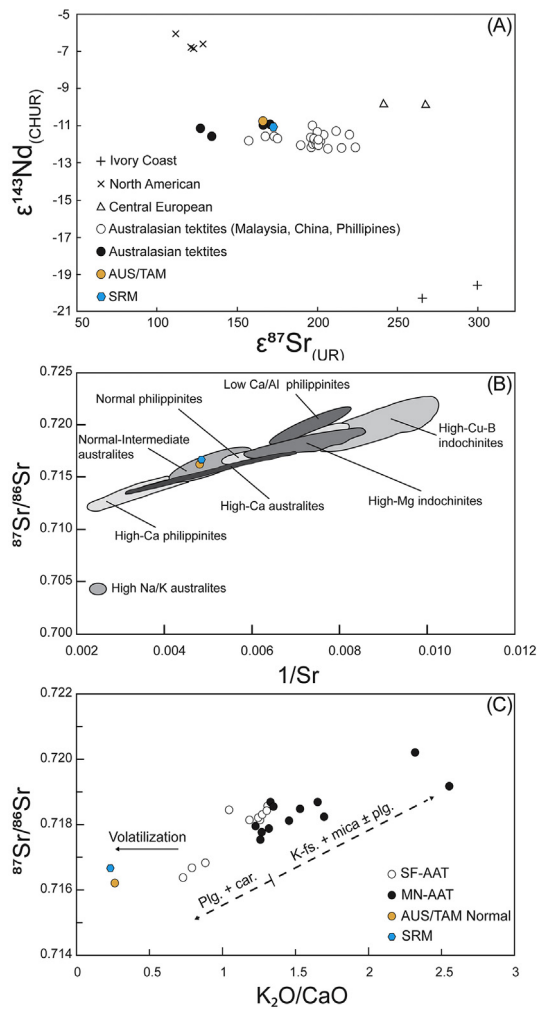
Fig. 7. Strontium and neodymium isotope plot. (A) $\varepsilon^{87}Sr_{UR}$ versus $\varepsilon^{143}Nd_{CHUR}$ diagram for (micro)tektites from the four major strewn fields. Values are expressed in the ε notation, where $\varepsilon^{87}Sr_{UR} = [(^{87}Sr/^{86}Sr)_{sample}/(^{87}Sr/^{86}Sr)_{UR} - 1] \times 10,000$ and $\varepsilon^{143}Nd_{CHUR} = [(^{143}Nd/^{144}Nd)_{sample}/(^{143}Nd/^{144}Nd)_{CHUR} - 1] \times 10,000$, UR = Uniform Reservoir, and CHUR = Chondritic Uniform Reservoir. The ε values of the SRM particles are consistent with literature values for the Australasian strewn field (Table 1). Reference values for Ivory Coast, North American, Central European and Australasian (micro)tektites from Shaw and Wasserburg (1982), Blum et al. (1992), Deutsch and Koeberl (2006), and Folco et al. (2009). Figure modified from Folco et al. (2009). (B) The Sr elemental and isotopic compositions of the SRM and Victoria Land particles appear to be consistent with reference values for normal- and intermediate-type australites. Reference values for Muong Nong-type and splash-form Australasian tektites from Compston and Chapman (1969), Shaw and Wasserburg (1982), Blum et al. (1992) and Lee et al. (2004). Figure modified from Ackerman et al. (2020). (C) $^{87}Sr/^{86}Sr$ versus K_2O/CaO diagram linking the respective (micro)tektites to a specific component within the target material. Australasian tektites displaying higher $^{87}Sr/^{86}Sr$ and K_2O/CaO presumably sampled a large proportion of K-feldspar, mica, and to a lesser extent plagioclase, due to the incorporation of radiogenic ^{87}Rb and K in the aforementioned mineral phases (Ackerman et al., 2020). In contrast, the lower abundances of ^{87}Rb and preferential incorporation of Ca and Sr in plagioclase and carbonate mineral phases consequently result in lower $^{87}Sr/^{86}Sr$ and K_2O/CaO ratios. Muong Nong-type tektites predominantly appear to have sampled the former lithology, while splash-form tektites are linked to both lithologies. The SRM and Victoria Land particles are positioned in a distinct location on the diagram, but have also suffered severe volatilization resulting in lower K_2O/CaO values, despite a similar $^{87}Sr/^{86}Sr$ ratio compared to splash-form tektites from Indonesia and the Philippines (Ackerman et al., 2020). The SRM and Victoria Land particles may therefore have sampled a plagioclase- and carbonate-rich target material assuming that the $^{87}Sr/^{86}Sr$ ratio did not change extensively as a result of volatilization. Figure modified from Ackerman et al. (2020).

suggested that average particle sizes may decrease as their distance from the source crater increases. The SRM particles range in size between 220 and 570 μm with an average size of ca. 370 μm, which also favors a trajectory path along the central, rather than the western,

distribution lobe. Due to low counting statistics for the SRM particles and Victoria Land microtektites of less than 400 μm in diameter, this interpretation should be considered with care. Potential effects from weathering processes can be excluded due to the lack of physicochemical alteration in the SRM particles across the entire size range (Fig. 8B–D). Significant sorting effects can also be discarded based on the physicochemical properties of the cosmic spherules extracted from the SRM sedimentary traps (cfr. See cumulative size distribution in Goderis et al., 2020) and TAM micrometeorites and microtektites (Suavet et al., 2009; Suttle and Folco, 2020).

(ii) Despite the substantial range of aerodynamic morphologies (e.g., spherical, dumbbell, teardrop, etc.) observed in Cenozoic microtektites (Glass et al., 2004), the vast majority of Victoria Land microtektites exhibits spherical shapes (ca. 98%; Folco et al., 2008, 2009). Folco et al. (2009) consequently suggested that the proportion of spherical tektites is positively correlated with distance from the source crater. This appears to be validated by the Larkman Nunatak microtektites where all 52 characterized microtektites exhibit spherical shapes (van Ginneken et al., 2018). The SRM particles also support these observations as 97% (32 out of 33) is spherical, with the exception of a single dumbbell-shaped particle (Fig. 8A–D). The latter displays a similar extent of volatile element depletion compared to its spherical counterparts, which suggests that the vaporization of volatile compounds occurs within the impact plume, rather than during atmospheric reentry, and is consistent with previous numerical models (e.g., Melosh, 1989; Artemieva et al., 2002).

(iv) The major and trace element geochemistry of the SRM particles is consistent with average compositions of upper continental crust, except for a number of elements including Na, K, V, Zn, Cs, Pb and U (Fig. 6). Volatile elements (i.e., Na, K, Cs, Pb, U) are partially vaporized during high thermal regimes and their loss passively enriches the more refractory elements (e.g., Zr, Hf, REE), as previously observed by Folco et al. (2009). The depletion of moderately volatile (e.g., Zn) and redox-sensitive elements (e.g., V, U) is more difficult to explain. These variations are likely primary in nature and may relate to target rock heterogeneity or variable redox conditions in the impact plume, but this cannot be further constrained based on the limited sample set. Given the pristine nature of the SRM particles, alteration processes are unlikely to have significantly affected the geochemical composition of the SRM particles.

(v) While seven polished sections were analyzed and imaged using SEM-EDS, no high SiO_2 inclusions have been observed in these particles. Folco et al. (2009) only reported a single lechatelierite inclusion among hundreds of Victoria Land microtektites, which Folco et al. (2010a) have argued to be a consequence of the high-temperature regime experienced by the Antarctic Australasian microtektites during the impact event (see discussion above). In addition, no vesicles have been observed in the SRM microtektites, which is consistent with the overall low number of vesicles observed in the Victoria Land and Larkman Nunatak microtektites (Folco et al., 2010a, 2016; van Ginneken et al., 2018).

(v) The H_2O content of (micro)tektites can also be utilized to discriminate the respective strewn fields (Glass et al., 2004). However, no water content was analyzed during this study due to the relative low number of particles recovered and priority to analyze the Sr–Nd isotopic compositions instead.

Based on the observations and arguments provided above, we propose that the SRM particles are microtektites affiliated to the Australasian strewn field. All recovered microtektites classify as 'normal-type' since the measured MgO concentrations are lower than 6 wt.% (Glass et al., 2004; Fig. 4 and Appendix A, Supplementary Data). Although the absence of the 'high-Mg' and 'intermediate-type' microtektites in the SRM collection may reflect a sampling or extraction bias, their abundance in other Australasian microtektite collections (5% to 10% by number; Glass et al., 2004; Folco et al., 2009) that were processed following comparable protocols, suggests that at least one such particle should be expected among the 33 SRM particles reported here. Their absence

Table 1

Rb–Sr and Sm–Nd elemental and isotopic compositions of the SRM-Victoria Land microtektites and Australasian tektites.

	Rb (µg/g)	Sr (µg/g)	$(^{87}Sr/^{86}Sr)_m \pm 2\sigma$	$\varepsilon^{87}Sr_{UR}$	Nd (µg/g)	Sm (µg/g)	$(^{143}Nd/^{144}Nd)_m \pm 2\sigma$	$\varepsilon^{143}Nd_{CHUR}$	T_{DM}^{Nd} (Ga)[1]	T_{DM}^{Nd} (Ga)[2]
SRM (n = 33)	32 ± 8	206 ± 19	0.716664 ± 12	173	43 ± 5	8.59 ± 1	0.512073 ± 10	−11.0	1.55	1.66
TAM – Sample A (n = 11)	38 ± 14	207 ± 35	0.716215 ± 10	166	42 ± 5	8.33 ± 1	0.512086 ± 29	−10.8	1.51	1.64
TAM – Sample B (n = 11)			0.716372 ± 10	168						
AAT – Muong Nong (n = 12)	116 ± 10	133 ± 12	0.717361–0.720206	183–223	33 ± 4	6.37 ± 1	0.512031–0.512062	−11.2 −11.8	1.49–1.57	1.67–1.71
AAT – Splash form (n = 10)	110 ± 9	132 ± 7	0.716361–0.718569	173–200	33 ± 2	6.31 ± 1	0.512035–0.512049	−11.5 −11.8	1.51–1.56	1.69–1.70

Note: Elemental concentrations and isotopic ratios are reported in ±1SD and ± 2σ, respectively. The $^{87}Sr/^{86}Sr$ and $^{143}Nd/^{144}Nd$ ratios of the SRM particles were measured on a batch of 26 particles (excluding WF-MT01–01 – WF-MT01–07). Average elemental concentrations (Rb, Sr, Nd, Sm) were calculated from all 33 SRM particles. Values reported for Muong Nong-type tektites include light-dark layers and bulk samples. The $\varepsilon^{87}Sr_{UR}$ values were calculated using the contemporary $^{87}Sr/^{86}Sr$ ratio (0.7045) of the Uniform Reservoir (Faure, 1986). The $\varepsilon^{143}Nd_{CHUR}$ values were calculated using the contemporary $^{143}Nd/^{144}Nd$ ratio (0.512638) of the Chondritic Uniform Reservoir (Wasserburg et al., 1981). [1]Single-stage Nd model age calculated using the $^{147}Sm/^{144}Nd$ (0.222) and $^{143}Nd/^{144}Nd$ (0.513114) reference values for the Depleted Mantle (DM) reservoir (Michard et al., 1985). [2]Two-stage Nd model age calculated using the $^{147}Sm/^{144}Nd$ (0.219) and $^{143}Nd/^{144}Nd$ (0.513151) reference values for the DM reservoir, and the $^{147}Sm/^{144}Nd$ (0.12) reference value for the continental crust (Liew and Hofmann, 1988). Reference values for Transantarctic Mountain (TAM) and Australasian tektites (AAT) reproduced from Folco et al. (2009) and Ackerman et al. (2020), respectively.

among the SRM microtektites may thus reflect initial compositional heterogeneity in the impact vapor plume or, alternatively, biases during transport from the impact site. Furthermore, we suggest that transportation of the SRM microtektites occurred along the central distribution lobe of the Australasian strewn field, which is supported by the extent of volatile element depletion and their size-frequency distribution (Figs. 8 and 9). This would extend the central distribution lobe toward the west and encompass the vast majority of the eastern Antarctic continent as well as the southeastern part of the Indian Ocean. These observations are also in agreement with previous studies, which position the hypothetical source crater on the Indochina peninsula (Barnes, 1964; Glass and Pizzuto, 1994; Ma et al., 2004; Prasad et al., 2007; Folco et al., 2010a, 2010b; Sieh et al., 2020).

4.2. Implications of the Sør Rondane Mountain microtektites

4.2.1. Revised distribution pattern of Australasian (micro)tektites and identification of potential recovery sites

The occurrence of microtektites in sediment traps from the SRM range is unique for the eastern Antarctic continent and substantially increases the total surface area of the Australasian strewn field up to 15% of the Earth's surface, verifying its status as one of the largest and most recent impact events on Earth. We have demonstrated that the Australasian strewn field extends west of the established field (Folco et al., 2008, 2009, 2016; van Ginneken et al., 2018) based on the physicochemical characteristics of the SRM microtektites, which presumably link these particles to the central distribution lobe of the Australasian strewn field. This may imply that additional sites in the southeastern Indian Ocean and on the eastern Antarctic continent can now be identified where the recovery of Australasian microtektites is plausible (Fig. 9B). This could potentially be tested by examining future ODP cores obtained from the southeastern Indian Ocean, or ice cores from the EPICA Dome C (or similar) ice record since their age has been demonstrated to be older (ca. 800 ka) than the Australasian impact event (e.g., Jouzel et al., 2007). Furthermore, due to the average smaller size and refractory nature of microtektites recovered from the Larkman Nunatak moraine, there is a possibility that similar types of these refractory microtektites can be recovered south of the SRM range. New sampling campaigns in surrounding (e.g., Mhlig-Hofmann) or western Antarctic (e.g., Ellsworth Mountains) mountain ranges may clarify whether this is the case. As such, the Australasian strewn field may encompass the whole Antarctic continent and Australasian microtektites could thus be used as a time-stratigraphic tracer in Antarctic ice cores. Furthermore, Australasian impact ejecta can provide a minimal age constraint of microtektite-bearing sedimentary traps (see e.g., Folco et al., 2008; Rochette et al., 2008; Genge et al., 2018). This may be useful to reconstruct the local/regional evolution of ice sheets on the Antarctic continent, as demonstrated by a case study in the Alan Hills by Folco et al.

(2016). The revised distribution pattern of Australasian (micro)tektites suggested in Fig. 9B maintains the established tri-lobe pattern, but is ultimately limited by the amount of ODP cores available (Glass and Simonson, 2013). As future ODP campaigns acquire new sediment cores from the southern Indian Ocean, the true extent of the Australasian strewn field can be constrained.

4.2.2. Abundance and preservation potential of Australasian microtektites in the Sør Rondane Mountains

Microtektite abundance in sedimentary traps from the SRM is surprisingly low. Here, we will use the Mt. Widerøe #01 sediment trap as example since the vast majority (ca. 82%) of microtektites were collected from this deposit. We estimate that <10 microtektites were recovered per kg of bulk detritus. In comparison, van Ginneken et al. (2018) estimate that the moraine deposits near Larkman Nunatak produced microtektite abundances on the order of ca. 200 per kg of sediment, while Folco et al. (2009) report even higher numbers of up to 400 per kg of sediment, which vary considerably between the different types of deposits. Even at some sites within the TAM, less than 1–2 microtektites were extracted per kg of sediment. Previous work has argued that the concentration of microtektites is mainly controlled by the erosion rate of the surrounding host rock and local environmental parameters, which may possibly affect sedimentary traps (Folco et al., 2009). The SRM sediment traps were sampled at altitudes ranging between ~2500 and 2800 m above sea level, which have not been affected by thaw throughout the year. Hence, we suggest that microtektites in the SRM deposits were predominantly diluted by variable erosion rates of the surrounding host rocks, rather than being subjected to weathering processes, or receiving lower numbers of Australasian microtektites. The deposits from the Mt. Widerøe #01 sediment trap are relatively coarse-grained and composed of gneissose biotite-hornblende metatonalite, which appear to be resilient to weathering in the cold and relatively dry Antarctic weather conditions (Goderis et al., 2020). In contrast, sediment traps from the Mt. Walnum #01 sampling site are more fine-grained and substantially weathered, and therefore only produce <1 microtektite per kg of bulk detritus. To maximize microtektite yields, sedimentary deposits should preferably be coarse-grained and resistant to alteration processes. This should prevent the dilution of microtektites through weathering of surrounding host rocks.

4.2.3. Target stratigraphy of the Sør Rondane and Transantarctic Mountain microtektites

Isotopic tracers, including the $^{87}Sr/^{86}Sr$ and $^{143}Nd/^{144}Nd$ ratios, are commonly used within impact cratering studies since (micro)tektites retain the isotopic signature of their target material. Consequently, these isotopic tracers are able to discriminate the respective (micro)tektite strewn fields (Fig. 7), but also allow to characterize their target material (Compston and Chapman, 1969; Shaw and Wasserburg, 1982;
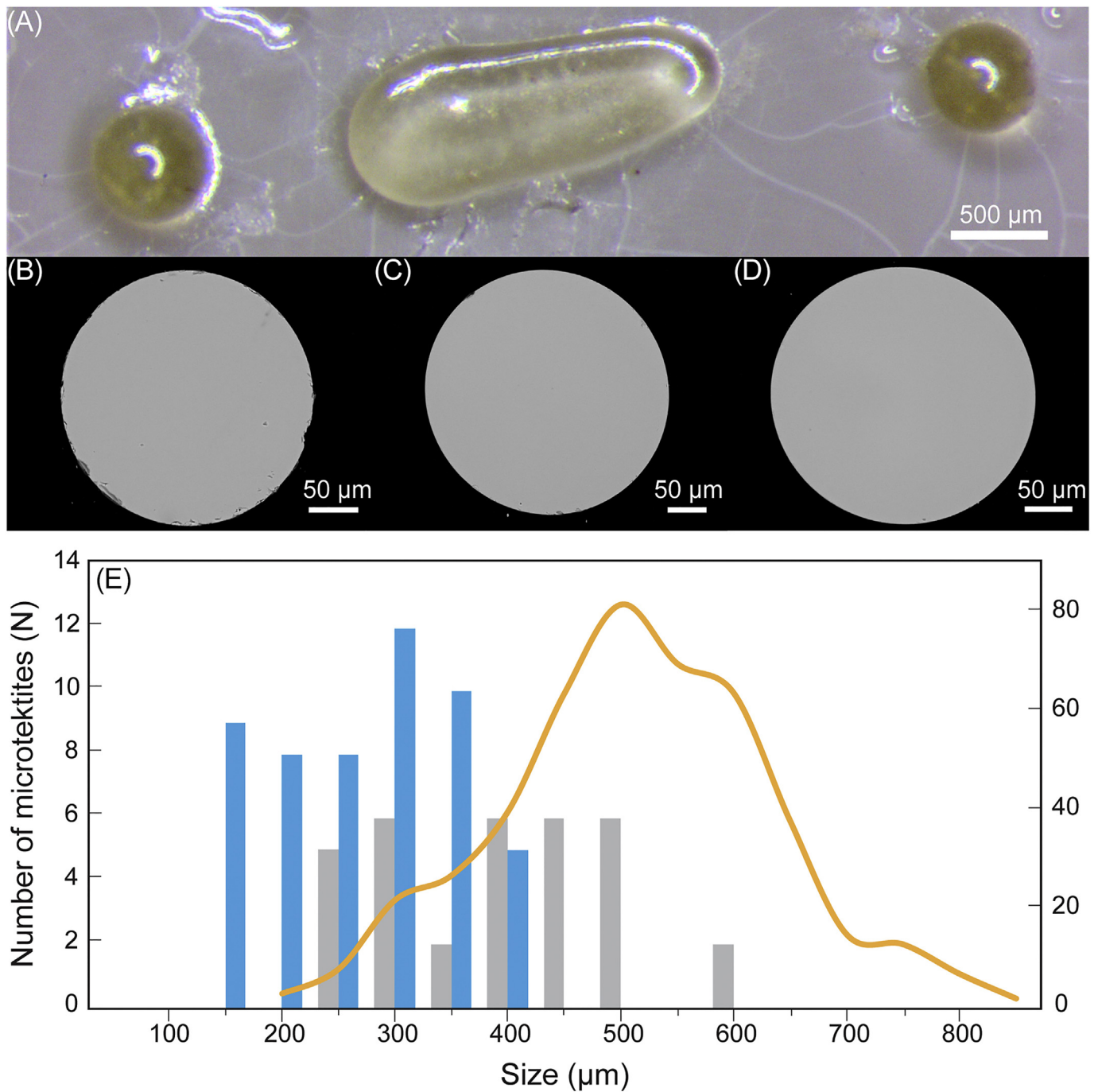
Fig. 8. Stereomicrograph (A) and BSE-SEM (B–D) images of the SRM microtektites. All particles display a typical pale yellow color and spherical shape, except for a single dumbbell-shaped particle (second particle in A, not shown in B). Particles are pristine and show only minor surficial fractures as observed from (B). Size-frequency distribution (E) of the SRM particles (this study), the Victoria Land microtektites (Folco et al., 2009), and Larkman Nunatak microtektites (van Ginneken et al., 2018). The frequency of the SRM particles and Larkman Nunatak microtektites is displayed on the left side of the y axis. The frequency of Victoria Land microtektites (curve) is displayed on the right side of the y axis. Despite the limited number of samples collected, the average size of the SRM particles (n = 33, size range of 220–570 μm) appears to be positioned in between those of Larkman Nunatak (n = 52, size range of 107–388 μm) and Victoria Land (n = 456, size range of 75–778 μm) (Folco et al., 2009; van Ginneken et al., 2018). Note that the size-frequency distribution of the SRM particles is biased for particles less than 200 μm, and less than 400 μm for Victoria Land microtektites due to limited sampling of these respective size fractions. Data reproduced from Folco et al. (2009) and van Ginneken et al. (2018).

Blum et al., 1992; Deutsch and Koeberl, 2006; Folco et al., 2009; Ackerman et al., 2020). The Nd isotope data observed in the SRM microtektites are intermediate between reference values of Australasian tektites and the Victoria Land microtektites (Fig. 7 and Table 1). This similarity, in conjunction with comparable $^{147}Sm/^{143}Nd$ values, has

been interpreted to reflect a fairly homogeneous target material for Australasian tektites with respect to the REE (Ackerman et al., 2020). The opposite pattern is observed for Sr isotopic ratios, which display a much larger range compared to the Nd isotope ratios. The distribution of Sr was likely controlled by variable proportions of both plagioclase
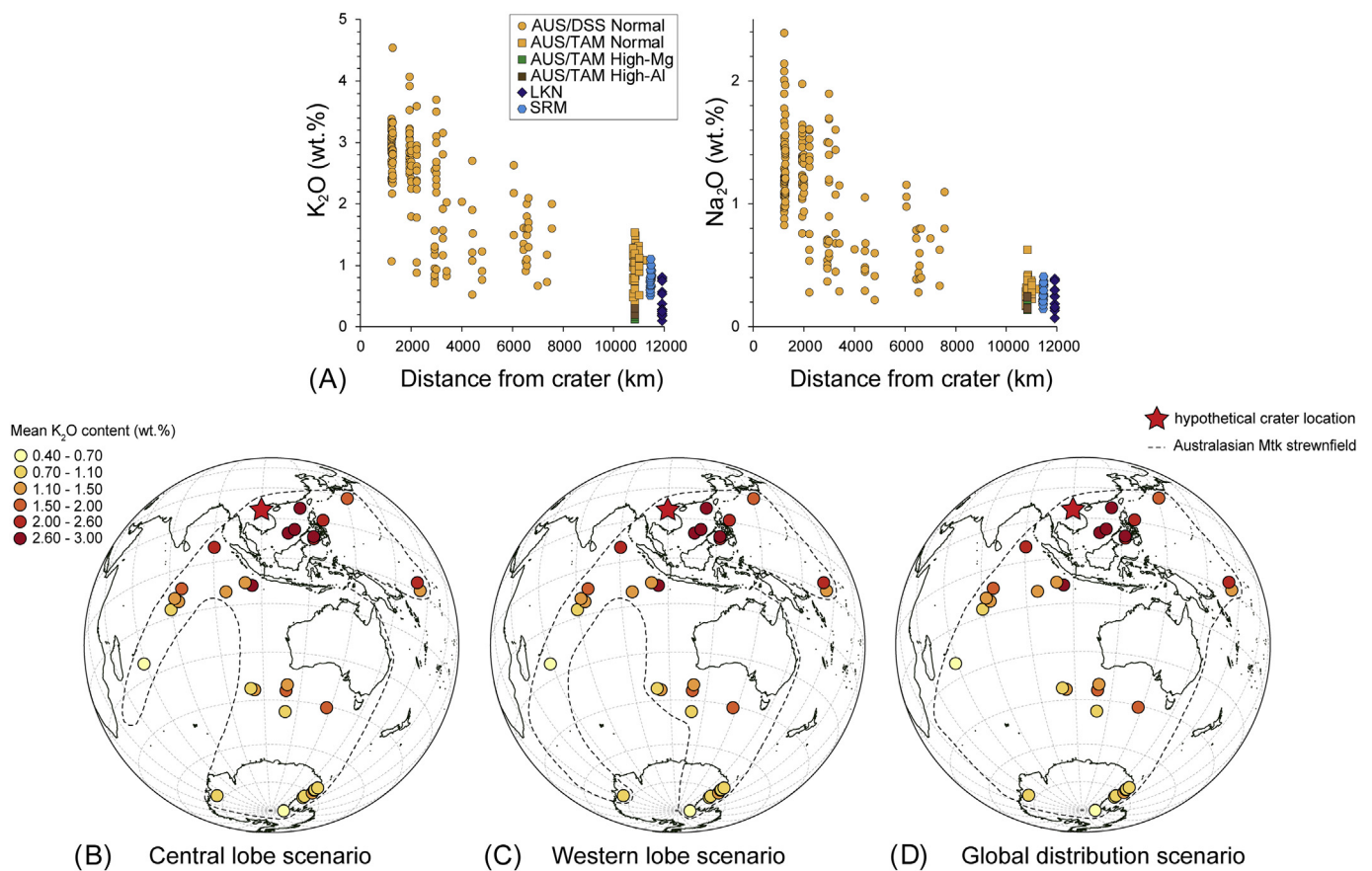
Fig. 9. (A) Distribution of volatile compounds (i.e., K_2O and Na_2O) in (micro)tektites across the Australasian strewn field (see Appendix A, Supplementary Data). On average, volatile element contents systematically decrease as distance from the hypothetical source crater increases. This is predominantly explained by high-temperature volatilization of target rock material during the impact event (Folco et al., 2010a), and was previously suggested for other volatile compounds (e.g., H_2O) by Artemieva et al. (2002). The source crater is assumed to be located on the Indochina peninsula following the observations of Barnes (1964), Glass and Pizzuto (1994), Ma et al. (2004), Prasad et al. (2007), Folco et al. (2010a, 2010b), Sieh et al. (2020). The range of measured volatile element contents of the SRM particles fall in between those from the Victoria Land and Larkman Nunatak microtektites. This is consistent with large-scale translation along the central distribution lobe of the Australasian strewn field. Figure modified from Folco et al. (2010a) and van Ginneken et al. (2018). (B–D) Hypothetical distribution pattern of the Australian strewn field including the SRM microtektites. Reference values for Australasian (micro)tektites from Cassidy et al. (1969), Glass et al. (2004), Glass and Koeberl (2006), Folco et al. (2010a), and van Ginneken et al. (2018). We argue that an extension of the central distribution lobe is more likely compared to the western distribution lobe as great circle distances along the latter trajectory path would exceed 13,000 km. This has also been suggested by Folco (2020) based on preliminary data reported in Soens et al. (2019). This would imply (on average) a more narrow size distribution and microtektite sizes, as well as extensive volatile compound depletion compared to the Larkman Nunatak microtektites. Instead, these parameters appear to be positioned between those of the Victoria Land and Larkman Nunatak microtektites. A global distribution scenario (as observed in D) is currently not supported due to the absence of Australasian microtektites in between the western and central distribution lobes, as demonstrated by previous ODP campaigns.

and K-feldspar (Ackerman et al., 2020). However, carbonates (calcite, dolomite) have also been detected in rock fragments from microtektite layers (Glass and Fries, 2008) and are also suggested based on high CaO contents (up to 10 wt.%) in a number of Australasian tektites from northern Australia (Compston and Chapman, 1969). Indeed, australites display the lowest $^{87}Sr/^{86}Sr$ values due to less radiogenic ingrowth from lower Rb/Sr values in the target lithologies.

Following discrete trends on a plot of $^{87}Sr/^{86}Sr$ versus K_2O/CaO, Ackerman et al. (2020) argued that splash-form tektites with slightly higher CaO contents reflect larger contributions of carbonate or plagioclase relative to Muong Nong-type tektites, and were derived from melting of the upper layers of a stratified sedimentary target at the Australasian impact site. Conversely, the Muong Nong-type tektites were thought to originate from melting of deeper, more heterogeneous parts of the target. Vertically stratified sediments deposited by a high-flux fluvial system capable of transporting and delivering silt-sized, rather well-homogenized sedimentary material, have previously been suggested and are both consistent with an impact site in the Gulf of Tonkin (e.g., Ma et al., 2004; Rochette et al., 2018; Whymark, 2018; Ackerman et al., 2019) or beneath the Bolaven volcanic field in Southern

Laos (Sieh et al., 2020). Both Antarctic data points fall within the cluster of splash-form australites and may suggest larger surficial target rock contributions (Fig. 7). This is consistent with ^{10}Be data for Victoria Land microtektites, which suggest that TAM microtektites were mainly sampled from the surface of the target material (i.e., soil, sediment) (Rochette et al., 2018, 2019). Based on the $^{87}Sr/^{86}Sr$ versus K_2O/CaO plot (Fig. 7C), this target material appears to be relatively plagioclase- and carbonate-rich. However, the K_2O/CaO ratio of the SRM and TAM microtektites is noticeably lower compared to splash-form tektites from Indonesia and the Philippines. This can presumably be attributed to volatilization where K (50% condensation temperature – $T_c \approx 1006$ K; Lodders, 2003) is predominantly vaporized over Ca (50% $T_c \approx 1517$ K). A plagioclase- and carbonate-rich target material is also consistent with the relatively CaO- and Sr-rich nature of the SRM and Victoria Land microtektites (Figs. 4, 6 and 7; Appendix A, Supplementary Data). Additionally, the moderately high condensation temperature of Sr (50% $T_c \approx 1464$ K; Lodders, 2003) suggests that potential effects of volatilization and mass-dependent fractionation should be minimal, thus reflecting the original target material composition. The correspondence in Sr and Nd isotope data for two geographical distinct Antarctic sites

therefore implies that the sedimentary target material was likely more effectively mixed during the generation of the Australasian microtektites.

5. Conclusions

Thirty-three microtektites were recovered from sedimentary traps in the SRM range (Queen Maud Land, East Antarctica). These particles are characterized by a typical pale yellow, transparent color and predominant spherical shapes (>97%). Microtektites range in size between ca. 224 and 558 μm with an average size of ca. 370 μm.Major and trace element chemistry largely overlaps with compositional data for 'normal-type' Australasian microtektites from Victoria Land, and strongly resembles average compositions of upper continental crust, except for a number of volatile elements. The physicochemical properties of the SRM microtektites, including the degree of volatile element depletion and its size-frequency distribution, are consistent with volatilization and particle size trends previously observed in the Victoria Land and Larkman Nunatak microtektites (Folco et al., 2009, 2010a, 2016; van Ginneken et al., 2018). The SRM microtektites thus appear to be affiliated to the Australasian strewn field, which is further supported by matching Nd and Sr isotope ratios falling on a mixing line typical for Australasian tektites. The central distribution lobe of the Australasian strewn field should therefore encompass a significantly larger geographical area including parts of the southeastern Indian Ocean and East Antarctica. The Australasian strewn field may extend across the entire Antarctic continent although this requires verification through dedicated sampling campaigns. If so, the presence of Australasian microtektites in sediments or ice layers can be used for time-stratigraphic correlation, as they display a unique geochemical composition and record of an instantaneous geological event across Antarctica. The SRM and Victoria Land microtektites display a remarkable similarity with Australasian tektites in terms of their Nd isotopic ratios, suggesting that the target material was homogenous in terms of the REE contents and was incorporated into a crustal unit of Paleo- or Mesoproterozoic age. Strontium isotopic ratios are more variable and suggest a contribution of plagioclase- or carbonate-rich target material. The abundance of microtektites in sedimentary traps from the SRM range appears to be controlled by the surrounding host rock lithology and its resistance to weathering. A higher contribution of microtektites is observed in coarse-grained lithologies, whereas fine-grained lithologies principally dilute microtektite abundances.

Declaration of competing interest

The authors declare that they have no known competing financial interests or personal relationships that could have appeared to influence the work reported in this paper.

Acknowledgements

Appendix A. Supplementary data

Supplementary data to this article can be found online at https://doi.org/10.1016/j.gsf.2021.101153.

References

Ackerman, L., Skála, R., Křížová, Š., Žák, K., Magna, T., 2019. The quest for an extraterrestrial component in Muong Nong-type and splash-form Australasian tektites from Laos using highly siderophile elements and Re-Os isotope systematics. Geochim. Cosmochim. Acta 56, 483–492. https://doi.org/10.1016/j.gca.2019.03.009.

Ackerman, L., Žák, K., Skála, R., Rejšek, J., Křížová, Š., Wimpenny, J., Magna, T., 2020. Sr-Nd-Pb isotope systematics of Australasian tektites: Implications for the nature and composition of target materials and possible volatile loss of Pb. Geochim. Cosmochim. Acta 276, 135–150. https://doi.org/10.1016/j.gca.2020.02.025.

Artemieva, N., Pierazzo, E., Stöffler, D., 2002. Numerical modeling of tektite origin in oblique impacts: implications to Ries-Moldavites strewn field. Bull. Czech Geol. Survey 77, 303–311.

Barnes, V.E., 1964. Variation of petrographic and chemical characteristics of indochinite tektites within their strewn-field. Geochim. Cosmochim. Acta 28, 893–913. https://doi.org/10.1016/0016-7037(64)90038-9.

Blum, J.D., Papanastassiou, D.A., Wasserburg, G.J., Koeberl, C., 1992. Neodymium and strontium isotopic study of Australasian tektites – New constraints on the provenance and age of the target materials. Geochim. Cosmochim. Acta 56, 483–492. https://doi.org/10.1016/0016-7037(92)90146-A.

Cassidy, W.A., Glass, B.P., Heezen, B.C., 1969. Physical and chemical properties of Australasian microtektites. J. Geophys. Res. 74, 1008–1025. https://doi.org/10.1029/JB074i004p01008.

Cavosie, A.J., Timms, N.E., Erickson, T.M., Koeberl, C., 2017. New clues from Earth's most elusive impact crater: evidence of reidite in Australasian tektites from Thailand. Geology 46, 203–206. https://doi.org/10.1130/G39711.1.

Chauvel, C., Blichert-Toft, J., 2001. A hafnium isotope and trace element perspective on melting of the depleted mantle. Earth Planet. Sci. Lett. 190, 137–151. https://doi.org/10.1016/S0012-821X(01)00379-X.

Compston, W., Chapman, D.R., 1969. Sr isotope patterns within the Southeast Australasian strewn-field. Geochim. Cosmochim. Acta 33, 1023–1036. https://doi.org/10.1016/0016-7037(69)90058-1.

Cordier, C., Folco, L., Taylor, S., 2011. Vestoid cosmic spherules from the South Pole Water well and Transantarctic Mountains (Antarctica): a major and trace element study. Geochim. Cosmochim. Acta 75, 1199–1215. https://doi.org/10.1016/j.gca.2010.11.024.

Cordier, C., Suavet, C., Folco, L., Rochette, P., Sonzogni, C., 2012. HED-like cosmic spherules from the Transantarctic Mountains, Antarctica: Major and trace element abundances and oxygen isotope compositions. Geochim. Cosmochim. Acta 77, 515–529. https://doi.org/10.1016/j.gca.2011.10.021.

Curzio, P., Folco, L., Laurenzi, M.A., Mellini, M., Zeoli, A., 2008. A tephra chronostratigraphic framework for the Frontier Mountain blue-ice field (northern Victoria Land, Antarctica). Quat. Sci. Rev. 27, 602–620. https://doi.org/10.1016/j.quascirev.2007.11.017.

Das Gupta, R., Banerjee, A., Goderis, S., Claeys, Ph., Vanhaecke, F., Chakrabarti, R., 2017. Evidence for a chondritic impactor, evaporation-condensation effects and melting of the Precambrian basement beneath the "target" Deccan basalts at Lonar crater, India. Geochim. Cosmochim. Acta 215, 51–75. https://doi.org/10.1016/j.gca.2017.07.022.

Deutsch, A., Koeberl, C., 2006. Establishing the link between the Chesapeake Bay impact structure and the north American tektite strewn field: the Sr-Nd isotopic evidence. Meteorit. Planet. Sci. 41, 689–703. https://doi.org/10.1111/j.1945-5100.2006.tb00985.x.

Faure, G., 1986. Principles of Isotope Geology. J. Wiley & Sons, Chichester, p. 589.

Folco, L., 2020. Antarctica: a treasure-trove for planetary sciences. Australasian microtektites from East Antarctica. 51st Lunar and Planetary Science Conference. Houston, Texas.

Folco, L., Rochette, P., Perchiazzi, N., D'Orazio, M., Laurenzi, M., Tiepolo, M., 2008. Microtektites from Victoria Land Transantarctic Mountains. Geology 36, 291–294. https://doi.org/10.1130/G24528A.1.

Folco, L., D'Orazio, M., Tiepolo, M., Tonarini, S., Ottolini, L., Perchiazzi, N., Rochette, P., Glass, B.P., 2009. Transantarctic Mountain microtektites: geochemical affinity with Australasian microtektites. Geochim. Cosmochim. Acta 73, 3694–3722. https://doi.org/10.1016/j.gca.2009.03.021.

Folco, L., Glass, B.P., D'Orazio, M., Rochette, P., 2010a. A common volatilization trend in Transantarctic Mountain and Australasian microtektites: implications for their formation model and parent crater location. Earth Planet. Sci. Lett. 293, 135–139. https://doi.org/10.1016/j.epsl.2010.02.037.

Folco, L., Perchiazzi, N., D'Orazio, M., Frezzotti, M.L., Glass, B.P., Rochette, P., 2010b. Shocked quartz and other mineral inclusions in Australasian microtektites. Geology 38, 211–214. https://doi.org/10.1130/G30512.1.

Folco, L., Bigazzi, G., D'Orazio, M., Balestrieri, M.L., 2011. Fission track age of Transantarctic Mountain microtektites. Geochim. Cosmochim. Acta 75, 2356–2360. https://doi.org/10.1016/j.gca.2011.02.014.

Folco, L., D'Orazio, M., Gemelli, M., Rochette, P., 2016. Stretching out the Australasian microtektite strewn field in Victoria Land Transantarctic Mountains. Polar Sci. 10, 147–159. https://doi.org/10.1016/j.polar.2016.02.004.

Folco, L., Glass, B.P., D'Orazio, M., Rochette, P., 2018. Impactor identification in Australasian microtektites based on Cr, Co and Ni ratios. Geochim. Cosmochim. Acta 222, 550–568. https://doi.org/10.1016/j.gca.2017.11.017.

Genge, M.J., van Ginneken, M., Suttle, M.D., Harvey, R.P., 2018. Accumulation mechanisms of micrometeorites in an ancient supraglacial moraine at Larkman Nunatak, Antarctica. Meteorit. Planet. Sci. 53, 2051–2066. https://doi.org/10.1111/maps.13107.

van Ginneken, M., Perchiazzi, N., Folco, L., Rochette, P., Bland, P.A., 2010. Meteoritic ablation debris from the Transantarctic Mountains: evidence for a Tunguska-like impact over Antarctica ca. 480 ka ago. Earth Planet. Sci. Lett. 293, 104–113. https://doi.org/10.1016/j.epsl.2010.02.028.

van Ginneken, M., Genge, M.J., Harvey, R.P., 2018. A new type of highly-vaporized microtektite from the Transantarctic Mountains. Geochim. Cosmochim. Acta 228, 81–94. https://doi.org/10.1016/j.gca.2018.02.041.

Glass, B.P., Fries, M., 2008. Micro-Raman spectroscopic study of fine-grained, shock-metamorphosed rock fragments from the Australasian microtektite layer. Meteorit. Planet. Sci. 43, 1487–1496. https://doi.org/10.1111/j.1945-5100.2008.tb01023.x.

Glass, B.P., Koeberl, C, 2006. Australasian microtektites and associated impact ejecta in the South China Sea and Middle Pleistocene supereruption of Toba. Meteorit. Planet. Sci. 41, 305–326. https://doi.org/10.1111/j.1945-5100.2006.tb00211.x.

Glass, B.P., Pizzuto, J.E., 1994. Geographic variation in Australasian microtektite concentrations: Implications concerning the location and size of the source crater. J. Geophys. Res. 99, 19075–19081. https://doi.org/10.1029/94JE01866.

Glass, B.P., Simonson, B.M., 2013. Distal Impact Ejecta Layers. A record of large impacts in sedimentary deposits. Springer-Verlag, Berlin, p. 716.

Glass, B.P., Wu, J., 1993. Coesite and shocked quartz discovered in Australasian and north American microtektite layers. Geology 21, 435–438. https://doi.org/10.1130/0091-7613(1993)021<0435:CASQDI>2.3.CO;2.

Glass, B.P., Huber, H., Koeberl, C., 2004. Geochemistry of Cenozoic microtektites and clinopyroxene-bearing spherules. Geochim. Cosmochim. Acta 68, 3971–4006. https://doi.org/10.1016/j.gca.2004.02.026.

Glass, B.P., Folco, L., Masotta, M., Campanale, F., 2020. Coesite in a Muong Nong-type tektite from Muong Phin, Laos: Description, formation, and survival. Meteorit. Planet. Sci. 55, 253–273. https://doi.org/10.1111/maps.13433.

Goderis, S., Tagle, R., Fritz, J., Bartoschewitz, R., Artemieva, N., 2017. On the nature of the Ni-rich component in splash-form Australasian microtektites. Geochim. Cosmochim. Acta 217, 28–50. https://doi.org/10.1016/j.gca.2017.08.013.

Goderis, S., Soens, B., Huber, M.S., McKibbin, S., van Ginneken, M., Van Maldeghem, F., Debaille, V., Greenwood, R.C., Franchi, I.A., Cnudde, V., Van Malderen, S., Vanhaecke, F., Koeberl, C., Topa, D., Claeys, Ph., 2020. Cosmic spherules from Widerøfjellet, Sør Rondane Mountains (East Antarctica). Geochim. Cosmochim. Acta 270, 112–143. https://doi.org/10.1016/j.gca.2019.11.016.

Jourdan, F., Nomade, S., Wingate, M.T.D., Eroglu, E., Deino, A., 2019. Ultraprecise age and formation temperature of the Australasian tektites constrained by ^{40}Ar/^{39}Ar analyses. Meteorit. Planet. Sci. 54, 2573–2591. https://doi.org/10.1111/maps.13305.

Jouzel, J., Masson-Delmotte, V., Cattani, O., Dreyfus, G., Falourd, S., Hoffmann, G., Minster, B., Nouet, J., Barnola, J.M., Chappellaz, J., Fischer, H., Gallet, J.C., Johnsen, S., Leuenberger, M., Loulergue, L., Luethi, D., Oerter, H., Parrenin, F., Raisbeck, G., Raynaud, D., Schilt, A., Schwander, J., Selmo, E., Souchez, R., Spahni, R., Stauffer, B., Steffensen, J.P., Stenni, B., Stocker, T.F., Tison, J.L., Werner, M., Wolff, E.W., 2007. Orbital and millennial Antarctic climate variability over the past 800,000 years. Science 317, 793–796. https://doi.org/10.1126/science.1141038.

Koeberl, C., 1994. Tektite origin by hypervelocity asteroidal or cometary impact: target rocks, source craters, and mechanism. In: Dressler, B.O., Grieve, R.A., Sharpton, V.L. (Eds.), Large Meteorite Impacts and Planetary Evolution. vol. 293. Geological Society of America Special Paper, pp. 133–151. https://doi.org/10.1130/SPE293-p133.

Lee, Y.T., Chen, J.C., Ho, K.S., Juang, W.S., 2004. Geochemical studies of tektites from East Asia. Geochem. J. 38, 1–17. https://doi.org/10.2343/geochemj.38.1.

Liew, T.C., Hofmann, A.W., 1988. Precambrian crustal components, plutonic associations, plate environment of the Hercynian Fold Belt of Central Europe: indications from a Nd and Sr isotopic study. Contrib. Mineral. Petrol. 98, 129–138. https://doi.org/10.1007/BF00402106.

Lodders, K., 2003. Solar system abundances and condensation temperatures of the elements. Astrophys. J. 591, 1220–1247. https://doi.org/10.1086/375492.

Ma, P., Aggrey, K., Tonzola, C., Schnabel, C., de Nicola, P., Herzog, G.F., Wasson, J.T., Glass, B.P., Brown, L., Tera, F., Klein, J., 2004. Beryllium-10 in Australasian tektites: constraints on the location of the source crater. Geochim. Cosmochim. Acta 68, 3883–3896. https://doi.org/10.1016/j.gca.2004.03.026.

Masotta, M., Peres, S., Folco, L., Mancini, L., Rochette, P., Glass, B.P., Campanale, F., Gueninchault, N., Radica, F., Singsoupho, S., Navarro, E., 2020. 3D X-ray tomographic analysis reveals how coesite is preserved in Muong Nong-type tektites. Sci. Rep. 10, 20608. https://doi.org/10.1038/s41598-020-76727-6.

Melosh, H.J., 1989. Impact Cratering. A Geological Process. Oxford Monographs on Geology and Geophysics No. 11. Oxford University Press, Oxford, p. 245.

Michard, A., Gurriet, P., Soudant, M., Albarède, F., 1985. Nd isotopes in French Phanerozoic shales: external vs. internal aspects of crustal evolution. Geochim. Cosmochim. Acta 49, 601–610. https://doi.org/10.1016/0016-7037(85)90051-1.

Montanari, A., Koeberl, C., 2000. Impact Stratigraphy. The Italian Record. Springer-Verlag, Berlin, p. 366.

Perchiazzi, N., Folco, L., Mellini, M., 1999. Volcanic ash bands in the Frontier Mountains and Lichen Hills blue ice fields, northern Victoria Land. Antarct. Sci. 11, 353–361. https://doi.org/10.1017/S0954102099000449.

Prasad, M.S., Mahale, V.P., Kodagali, V.N., 2007. New sites of Australasian microtektites in the Central Indian Ocean: implications for the location and size of source crater. J. Geophys. Res. 112, E06007. https://doi.org/10.1029/2006JE002857.

Rochette, P., Folco, L., Suavet, C., van Ginneken, M., Gattacceca, J., Perchiazzi, N., Braucher, R., Harvey, R.P., 2008. Micrometeorites from the Transantarctic Mountains. Proc. Natl Acad. Sci. USA 105, 18206–18211. https://doi.org/10.1073/pnas.0806049105.

Rochette, P., Braucher, R., Folco, L., Horng, C.S., Aumaître, G., Bourlès, D.L., Keddadouche, K., 2018. ^{10}Be in Australasian microtektites compared to tektites: size and geographic controls. Geology 46, 803–806. https://doi.org/10.1130/G45038.1.

Rochette, P., Braucher, R., Folco, L., Horng, C.S., Aumaître, G., Bourlès, D.L., Keddadouche, K., 2019. ^{10}Be in Australasian microtektites compared to tektites: size and geographic controls. Geology 47, e460. https://doi.org/10.1130/G46156Y.1.

Schwarz, W.H., Trieloff, M., Bollinger, K., Gantert, N., Fernandes, V.A., Meyer, H.-P., Povenmire, H., Jessberger, E.K., Guglielmino, M., Koeberl, C., 2016. Coeval ages of Australasian, central American and Western Canadian tektites reveal multiple impacts 790 ka ago. Geochim. Cosmochim. Acta 178, 307–319.

Shaw, H.F., Wasserburg, G.J., 1982. Age and provenance of the target materials for tektites and possible impactites as inferred from Sm-Nd and Rb-Sr systematics. Earth Planet. Sci. Lett. 60, 155–177. https://doi.org/10.1016/0012-821X(82)90001-2.

Sieh, K., Herrin, J., Jicha, B., Schonwalder, Angel D., Moore, J.D.P., Banerjee, P., Wiwegwin, W., Sihavong, V., Singer, B., Chualaowanich, T., Charusiri, P., 2020. Australasian impact crater buried under the Bolaven volcanic field, Southern Laos. Proc. Natl. Acad. Sci. U. S. A. 117, 1346–1353. https://doi.org/10.1073/pnas.1904368116.

Soens, B., van Ginneken, M., Debaille, V., Vanhaecke, F., Claeys, Ph., Goderis, S., 2019. Microtektites from the Sør Rondane Mountains, East Antarctica: Towards an extension of the Australasian strewn field? 82nd Annual Meeting of the Meteoritical Society. Sapporo, Japan

Suavet, C., Rochette, P., Kars, M., Gattacceca, J., Folco, L., Harvey, R.P., 2009. Statistical properties of the Transantarctic Mountains (TAM) micrometeorite collection. Polar Sci. 3, 100–109. https://doi.org/10.1016/j.polar.2009.06.003.

Suganuma, Y., Miura, G.-H., Zondervan, A., Okuno, J., 2014. East Antarctic deglaciation and the link to global cooling during the Quaternary: evidence from glacial geomorphology and ^{10}Be surface exposure dating of the Sør Rondane Mountains, Dronning Maud Land. Quat. Sci. Rev. 97, 102–120. https://doi.org/10.1016/j.quascirev.2014.05.007.

Suttle, M.D., Folco, L., 2020. The extraterrestrial dust flux: Size distribution and mass contribution estimates inferred from the Transantarctic Mountains (TAM) micrometeorite collection. J. Geophys. Res. Planets 125. https://doi.org/10.1029/2019JE006241.

Taylor, S., Herzog, G.F., Delaney, J.S., 2007. Crumbs from the crust of Vesta: Achondritic cosmic spherules from the south Pole water well. Meteorit. Planet. Sci. 42, 223–233. https://doi.org/10.1111/j.1945-5100.2007.tb00229.x.

Taylor, S.R., McLennan, S.M., 1995. The geochemical evolution of the continental crust. Rev. Geophys. 33, 241–265. https://doi.org/10.1029/95RG00262.

Walter, L.S., 1965. Coesite discovered in tektites. Science 147, 1029–1032. https://doi.org/10.1126/science.147.3661.1029.

Wasserburg, G.J., Jacobsen, S.B., DePaolo, D.J., McCulloch, M.T., Wen, T., 1981. Precise determination of Sm/Nd ratios, Sm and Nd isotopic abundances in standard solutions. Geochim. Cosmochim. Acta 45, 2311–2324. https://doi.org/10.1016/0016-7037(81)90085-5.

Weis, D., Kieffer, B., Maerschalk, C., Barling, J., de Jong, J., Williams, G.A., Hanano, D., Pretorius, W., Mattielli, N., Scoates, J.S., Goolaerts, A., Friedman, R.M., Mahoney, J.B., 2006. High-precision isotopic characterization of USGS reference materials by TIMS and MC-ICP-MS. Geochem. Geophys. Geosyst. 7, 1–30. https://doi.org/10.1029/2006GC001283.

Whymark, A., 2018. Further geophysical data in the search for the Australasian tektite source crater location in the Song Hong – Yinggehai Basin, Gulf of Tonkin. 49th Lunar and Planetary Science Conference. Texas, Houston.